THE JOURNAL OF BIOLOGICAL CHEMISTRY VOL. 282, NO. 35, pp. 25299–25307, August 31, 2007

N-Methyl-D-aspartate (NMDA) Receptor Subunit NR1 Forms the Substrate for Oligomeric Assembly of the NMDA Receptor*

Received for publication, April 2, 2007, and in revised form, July 2, 2007 Published, JBC Papers in Press, July 2, 2007, DOI 10.1074/jbc.M702778200

Palmi T. Atlason[‡], Molly L. Garside[§], Elisabeth Meddows[¶], Paul Whiting[¶], and R. A. Jeffrey McIlhinney[‡1]

From the [‡]MRC Anatomical Neuropharmacology Unit, Mansfield Road, Oxford OX1 3TH, [¶]Merck Sharp & Dohme Neuroscience Research Centre, Terlings Park, Eastwick Road, Harlow, Essex CM20 2QR, and the [§]School of Biological Sciences, Royal Holloway College, University of London, Egham TW20 0EX, United Kingdom

The time course of the assembly of the *N*-methyl-D-aspartate receptor was examined in a cell line expressing it under the control of the dexamethasone promoter. These studies suggested a delay between the appearance of the NR1 and NR2A subunits and their stable association as examined by co-immunoprecipitation of NR1 and NR2A. This prompted us to examine the stability and folding of the individual subunits using nonreduced polyacrylamide gels and the sulfhydryl cross-linker BMH. Both studies showed that the NR1 subunit was expressed in a monomer and dimer form, whereas both NR2 and NR3 showed substantial aggregation on both nonreduced gels and after cross-linking. Protein degradation experiments showed that NR1 was relatively stable, whereas NR2 and NR3 were more rapidly degraded. When co-expressed with NR1, NR2 was more stable. Fluorescence recovery after photobleaching experiments showed that, under conditions of reduced ATP, the diffusion rate of NR2 and NR3 in the endoplasmic reticulum was reduced, whereas that of NR1 was unaffected. Together these data show that NR1 folds stably when expressed alone, unlike NR2 and NR3, and provides the substrate for assembly of the *N*-methyl-D-aspartate receptor.

The N-methyl-D-aspartate (NMDA)[2] receptor subtype of the glutamate receptor family are hetero-oligomeric proteins composed of three classes of receptor subunits: NR1, NR2, and NR3. The NR1 subunit is encoded by a single gene, which undergoes extensive splicing to generate eight different splice variants that differ in regional distribution and functional properties (1). The NR2 subunit class consists of four different subtypes, NR2A–NR2D, encoded by four separate but closely related genes (reviewed in Ref. 1). The NR3 subunit class consists of two different subtypes, NR3A and NR3B (2–4). A number of studies of mammalian cell lines either permanently or transiently transfected with the NMDA receptor subunits have indicated that the NR1 subunit alone does not form glycine-glutamate responsive channels and requires the presence of NR2 (5–7). Other studies have shown that the NR1 and NR2 subunits contribute differently to the binding sites of a functional NMDA receptor. The NR1 subunit forms the glycine binding site (8, 9), and the NR2 subunit provides part of the glutamate binding site (10, 11). Similar studies on the NR3 subunit family suggested that it could act as a dominant negative subunit that reduced channel conductances when associated with NR1 and NR2 (4, 12). However, several recent studies have suggested that NR3 can combine with NR1 alone to form an excitatory glycine channel in both transfected cells and the central nervous system (13–15). Thus, different combinations of the NMDA receptor subunits must co-assemble to form functionally distinct ion channels.

Current evidence indicates that the glutamate-activated ion channels are tetrameric. Biochemical and biophysical evidence from studies on α-amino-3-hydroxy-5-methyl-4-isoxazolepropionate receptors strongly support such a structure (16). These studies also indicate that the assembly of the receptor is by the association of already dimerized subunits (16–18). Because the NMDA receptors are members of the same gene family as the α-amino-3-hydroxy-5-methyl-4-isoxazolepropionate receptors, and x-ray crystallographic studies of the soluble ligand binding domains of both receptors reveal similar structures, it is likely that the NMDA receptor is also a tetramer (19–21). However, it is unclear how the NMDA receptor is assembled or whether it too forms by association of dimers of the different subunits. Studies using tandem chimaeras of the NR1 and NR2 subunits suggested that a dimer of dimers model could account for the assembly of the NMDA receptor (22), but evidence for the formation of dimers of the different subunits is scarce. In a study of the determinants important for NMDA receptor assembly (23), we found that NR1 subunits expressed alone in HEK-293 cells ran as dimers on native gels. In contrast, NR2 subunits expressed alone gave a smear of immunoreactivity suggesting that they were not folding stably. Interestingly, a recent report suggests that an N-terminal NR1-NR1 interdisulfide bond is necessary for the trafficking of the NMDA receptor to the cell surface (24).

To investigate the assembly pathway of the human NMDA receptor we have examined the time course of the assembly of the receptor in a cell line expressing it under the control of the dexamethasone promoter. These studies revealed an unexpected delay between the appearance of the subunits and their association as judged by co-immunoprecipitation of NR1 and NR2. This prompted us to examine the stability and folding of the individual subunits using nonreduced polyacrylamide gels and the sulfhydryl cross-linker BMH, together with fluorescence recovery after photobleaching (FRAP) analysis of their

* The costs of publication of this article were defrayed in part by the payment of page charges. This article must therefore be hereby marked "*advertisement*" in accordance with 18 U.S.C. Section 1734 solely to indicate this fact.

[1] To whom correspondence should be addressed: Tel.: 44-1865-271-896; Fax: 44-1865-271-647; E-mail: jeff.mcilhinney@pharm.ox.ac.uk.

[2] The abbreviations used are: NMDA, *N*-methyl-D-aspartate; BMH, bismaleimidohexane; FRAP, fluorescence recovery after photobleaching; HA, hemagglutinin; YFP, yellow fluorescent protein; PBS, phosphate-buffered saline; BN-PAGE, blue native-PAGE; Bis-Tris, 2-[bis(2-hydroxyethyl)amino]-2-(hydroxymethyl)propane-1,3-diol; ER, endoplasmic reticulum.

diffusion rate in the endoplasmic reticulum. All data were consistent with the NR1 subunit being stably folded and expressed in a monomer and dimer form. In contrast both NR2 and NR3 showed substantial aggregation on both nonreduced gels and after cross-linking and rapid rates of degradation compared with NR1, suggesting that they fold less well and are, consequently, less stable than NR1. The stability of NR2 was increased when co-expressed with NR1. The results are consistent with NR1 folding stably when expressed alone and providing a substrate for the stable association and folding of the other subunits into functional NMDA receptors.

MATERIALS AND METHODS

Antibodies—The NR2A subunit was detected using a rabbit anti-NR2A antibody raised against the C terminus of NR2A as previously described (25). The NR1-1a subunit was detected using antibodies raised against the C terminus as previously described (25). The anti-myc mouse monoclonal antibody clone 9E10 was produced in-house from a hybridoma, and the rabbit anti-HA antibody was supplied by BabCO, Berkeley, CA. To produce an antibody against the NR3A subunit, the last 160 amino acids of NR3A (Tyr^{956}–Ser^{1116}) were amplified by PCR and cloned into the pET32a vector to produce a thioredoxin fusion protein containing a His_6 tag followed by a thrombin cleavage site and the sequence from the C terminus of NR3A. The protein was expressed in *Escherichia coli* BL21 cells and then purified on a Talon nickel chelate column (Clontech, Mountain View, CA). The fusion peptide was released from the fusion protein by thrombin cleavage, purified, and used to immunize New Zealand White rabbits. The immunopositive sera were further affinity-purified using the fusion protein coupled to a Sulfo-link column (Pierce), and the antibodies were recovered using 50 mM glycine, pH 2.5, followed by immediate neutralization with 1 M Tris. The specificity of the affinity purified antibodies was tested using membranes from cells expressing NR1-1A, NR2A, and NR3A subunits, and no immunoreactivity was found with NR1 or NR2 subunits. In rat brain membranes the affinity-purified antibodies gave a single immunoreactive band at 130 kDa that showed the developmental expression profile reported for NR3A in rats (26). The primary antibodies were detected using a 1:5000 dilution of donkey anti-sheep (Sigma-Aldrich), goat anti-rabbit, or goat anti-mouse antibodies conjugated to horseradish peroxidase (Promega, Madison, WI).

Recombinant Constructs—The human NMDA receptor subunits NR1-1a, NR2A, NR3A, and HA-tagged NR3A were kindly provided by Dr. Paul Whiting and Dr. Peter Wingrove of Merck Sharp and Dohme. The NR1Δ843 construct has been described previously (23). NR1-1a fused at the C terminus with yellow fluorescent protein (YFP) was produced by PCR using KOD HiFi polymerase (Novagen, Nottingham, Nottshire, UK) and the primers 5′-CCAGTGTGCTGGAATTCCCGCGCC-3′ and 5′-GCGGGCGGGGTCGACCAGCTCTCCCTAT-3′. The PCR product was digested with EcoRI and SalI and ligated into a similarly digested pEYFP-N1 vector (Clontech). NR3A C-terminally linked to YFP was produced in the same way but using the primers 5′-CGCGCTTTCTCCAAGCTTGTCTCAGTAATG-3′ and 5′-GTCAGGGACGTGAATTCGGTACTTAAGGG-3′ followed by digestion of the PCR product with HindIII and EcoRI. C-terminally linked NR2A-YFP was produced by ligation of the PCR product produced by amplification of the NR2A using the primers 5′-CTAGAGACAAGATCTACACTATAGATG-3′ and 5′-GGAAGAAGATCTACATCAGATTCGATACTAGGCAT-3′ and digestion of the product with BglII. The digested insert was ligated into BglII-digested eYFP-N1. Myc-tagged NR2AΔ848 was similarly created using the primers 5′-CGAAATTAATACCAGTGGTACCTATGGGCAGAGTC-3′ and 5′-GTCGGAGCACACGCCCTCGAGACAGAAGCGCAGC-3′. The resulting PCR product was then digested with KpnI and XhoI and ligated into a similarly digested pCDNA3.1*myc*HisA(+) vector.

Myc-tagged NR2AΔ890 was created as follows using the NR2A in pcDNA1.1 described previously (23). NR2A was digested with HindIII and BamHI to yield a ~1300-bp fragment comprising residues 465–890 of NR2A, which was ligated into similarly digested pcDNA3.1*myc*HisB(+) vector (Invitrogen). Subsequently, a ~1400-bp fragment comprising residues 1–464 of NR2A was removed from the original NR2A vector using HindIII. This fragment was ligated into HindIII-digested $NR2A_{456-890}$ in pcDNA3.1*myc*HisB(+) to yield the *myc*-His-tagged NR2AΔ890. The truncated subunit was C-terminally YFP-tagged by amplifying the YFP-encoding fragment from eYFP-N1 vector with the forward primer 5′-GCTACCGGACTCAGATCTCGAGCTCAAGCTTCG-3′ and reverse primer 5′-GTGCCGCGGCTGATTATGATCTAGAGTCG-3′, which introduces a SacII site. The resulting PCR product was digested with SacII and ligated into a similarly digested NR2AΔ890 in pcDNA3.1*myc*HisB-(+) to create NR2AΔ890-YFP. The fidelity of all constructs was confirmed by DNA sequencing.

Cell Culture and Transfection—HEK-293 and COS-7 cells were grown in Dulbecco's modified Eagle's medium (Sigma) supplemented with 10% (v/v) fetal calf serum (Invitrogen), 2 mM L-glutamine, 50 units/ml penicillin, 50 μg/ml streptomycin (all from Invitrogen) at 37 °C, in humidified atmosphere of 5% CO_2. For microscopy the cells were plated onto glass coverslips. Cells were transfected using JetPEI, a polyethyleneimine-derived transfection reagent (Autogen Bioclear, Calne, Wiltshire, UK), according to the manufacturer's instructions. In co-expression experiments with NR1 and NR2 or NR3 the ratio of DNAs was 1:3.

The stably transfected mouse connective tissue fibroblast L(tk−) cell line expressing recombinant human NR1-1a/NR2A receptor subunits under the control of the dexamethasone promoter system has been described previously (27). The cell line was grown in 75-cm^2 flasks in Dulbecco's modified Eagle's medium, supplemented with 2 mM L-glutamine, 10% (v/v) fetal calf serum, 100 units/ml penicillin, and 1 mg/ml Geneticin (PAA Laboratories, Pasching, Austria), at 37 °C in an atmosphere of 5% CO_2. Expression of NR1-1a and NR2A subunits was induced by addition of 1 μM dexamethasone (in methanol) to the growth medium. The excitotoxicity encountered when expressing recombinant NMDA receptors in mammalian cells was overcome by the addition of ketamine (0.5 mM) to the culture medium after induction. For metabolic labeling of cells

with [^{35}S]methionine (Amersham Biosciences), the L(tk−) cell line was plated onto 6-well plates and after 24 h induced to express the NMDA receptor. After 24-h induction the cells were incubated in methionine-free medium for 40 min before adding [^{35}S]methionine (100 μCi/ml) for 15 min. The cells were then washed with full medium twice, followed by two more washes with phosphate-buffered saline, then lysed and immunoprecipitated for NR1 as described below.

Co-immunoprecipitation—The L(tk−) cells were grown for 48 h then induced and processed at time points 0–8 h by quantitative co-immunoprecipitation and analyzed using SDS-PAGE, as described previously in detail (23). HEK-293 cells were transfected as described above and cultured for 48 h before use. Briefly, cells were lysed on ice with 1 ml of RIPA buffer (50 mM Tris-HCl, pH 7.5, 1% (w/v) Triton X-100, 0.5% sodium deoxycholate, 0.1% SDS, 100 mM NaCl, 1 mM EDTA) plus the complete protease inhibitor mixture (Roche Diagnostics, Mannheim, Germany) and 20 mM iodoacetamide. Samples of the lysate were rotated overnight at 4 °C with 2–5 μg of the appropriate antibodies. A 100-μl suspension of Protein G-Sepharose Fast-Flow beads (GE Healthcare, Uppsala, Sweden) was added to the precipitates and mixed by rotation at 4 °C for 2 h. The immunoprecipitates were pelleted by centrifugation, and the resulting pellet was washed twice in RIPA buffer then twice with 50 mM Tris-HCl, pH 8.0. The immunocomplexes were eluted from the Protein G beads by boiling in 2× reducing sample buffer (20 mM dithiothreitol, 2% (w/v) SDS, 10% (v/v) glycerol, 100 mM Tris-HCl). Both the precipitates and total cell lysates were analyzed by SDS-PAGE and Western immunoblot. In the case of the immunoprecipitates from the radiolabeled cells, the gels were impregnated with Fluor and subjected to autoradiography as described previously (25).

Cross-linking and Cycloheximide Treatment of Cells—Bismaleimidohexane (BMH), a sulfhydryl-specific cross-linker with a 16.1-Å linker arm, was purchased from Pierce. A 50 mM stock solution of BMH in Me_2SO was freshly prepared on day of the experiment. It was then diluted in PBS with 1% Triton X-100 to give a 2.5 mM working solution (lysis buffer). HEK-293 cells transiently transfected with the different subunits were scraped from the 6-well plates in PBS, centrifuged (5000 rpm, 5 min at room temperature), lysed with lysis buffer, and incubated in the dark at room temperature for 45 min, with occasional mixing by inversion. Excess BMH was quenched by adding an equal volume of 2× reducing sample buffer and incubating for a further 10 min. Samples were then heated to 99 °C for 5 min, and 50-μl samples of the lysates were analyzed by SDS-PAGE as described below.

For the degradation experiments, cycloheximide (Sigma) was dissolved in Me_2SO to create a 50 mg/ml stock solution. HEK-293 cells were transiently transfected with the indicated NMDA receptor subunits in 25-cm^2 flasks and grown for 24 h. They were then re-plated into 6-mm wells and grown for another 24 h. Rat cortical neurons were harvested at E19 as described previously (28) and grown for 14 days *in vitro* before cycloheximide treatment. Cycloheximide was added to a final concentration of 50 μg/ml, and cells were harvested by scraping into PBS, spinning down, and lysing in 150 μl of 2× reducing sample buffer at the indicated time points. Samples (45 μl) were analyzed on SDS-PAGE gels, and the immunoreactive bands were quantified using the Quantity One software supplied with the FluorSmax Imager (Bio-Rad). Western blotting for tubulin was performed to ensure even loading of samples.

For the lactacystin (Sigma) experiments, HEK-293 cells were transfected and seeded as described for the cycloheximide experiments. Lactacystin was added to the wells from a 1 mM stock solution in H_2O to a final concentration of 10 μM, and cells were incubated for 16 h. Samples were analyzed as described for the cycloheximide experiments.

Western Immunoblotting—Proteins were separated by SDS-PAGE using 6% or 7.5% polyacrylamide gels under reducing or nonreducing conditions. After transfer to nitrocellulose or polyvinylidene fluoride membrane (PerkinElmer Life Sciences) using a Trans blot semi-dry transfer cell (Bio-Rad) the membranes were blocked in 5% (w/v) nonfat dried milk in PBS/0.05% Tween 20 (PBS-T) for 1 h. The primary antibodies were incubated with the immunoblots overnight at 4 °C and subsequently detected using horseradish peroxidase-conjugated secondary antibodies in conjunction with the chemiluminescence SuperSignal kit (Pierce).

Blue Native-PAGE—The oligomeric structure of native protein complexes was analyzed using a modification of BN-PAGE, as described previously (23, 29, 30). Briefly, membrane samples were prepared by mixing with 1 mg/ml DNase (with 10 mM $CaCl_2$ and 10 mM $MgCl_2$), and the mixture was incubated at room temperature for 15 min. An equal volume of 2× BN-PAGE sample buffer (200 mM Bis-Tris, 150 mM 6-amino caproic acid, 2% Triton X-100, pH 7) was added to each sample, and the mixture was incubated on ice for 15 min. The membrane samples were centrifuged at 100,000 × *g* for 45 min and mixed with 5% Serva blue dye. The markers thyroglobulin, bovine serum albumin, apoferritin, and β-amylase were mixed with 5% Serva blue dye and run with the samples on a 5–18% gel containing no detergent. The samples and markers were stacked at 100 V, then run at 500 V and 15 mA at 4 °C. The gel was then subjected to a revised Western immunoblot protocol. The marker lanes were stained with Coomassie Blue dye (50% methanol, 10% acetic acid, 0.2% (w/v) Coomassie Blue) then destained to visualize the protein bands. The section of the membrane containing the proteins was washed with PBS-T and processed as described for the SDS-PAGE immunoblots.

FRAP Analysis—COS-7 cells were transiently transfected with the different NMDA receptor subunits tagged at the C terminus with YFP. Fluorescence recovery after photobleaching (FRAP) was recorded using a Zeiss LSM-510 confocal microscope essentially as described previously (31). Briefly, YFP was bleached with a high power laser beam (17 milliwatts) and recovery into the bleached area monitored for 2 min. Recovery is presented as percentage of original fluorescence, corrected for any bleaching due to repetitive scanning, at 1% of total laser output. Cells were depleted for ATP by incubating for 60 min at 37 °C in Hanks' balanced salt solution with 50 μM 2-deoxyglucose and 0.02% sodium azide, which reduced the ATP content of the cells by 75% (data not shown). The FRAP data were best fitted to a single exponential using IGOR PRO software and the FRAP plug-in written by K. Miura. Statistical analysis of the FRAP data was performed in GraphPad Prism

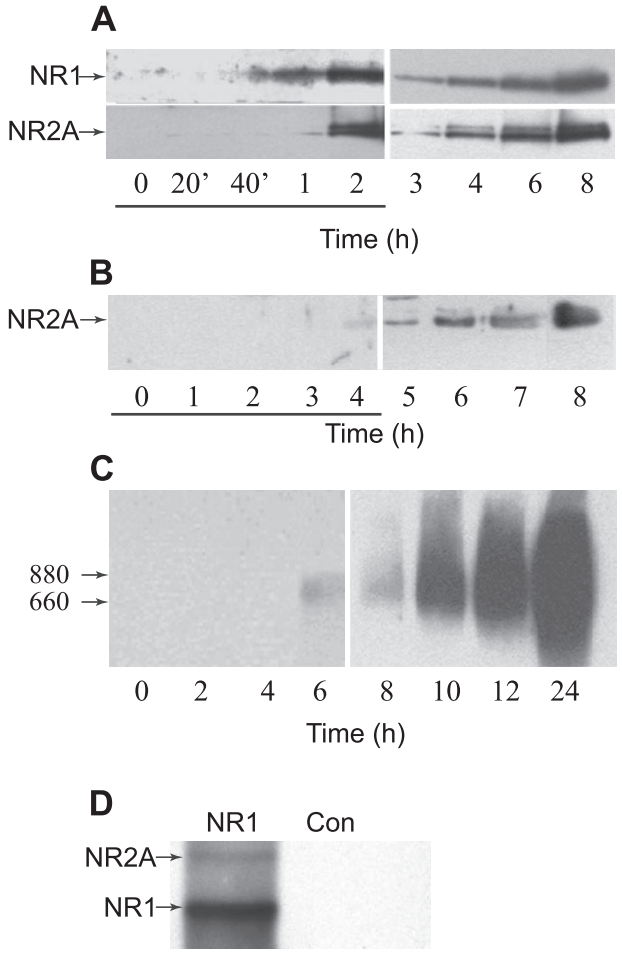

FIGURE 1. **Analysis of NMDA receptor assembly in induced L(tk−) cells.** *A*, L(tk−) cells were induced to express the NMDA receptor by the addition of 5 μM dexamethasone. At the indicated times post-induction the cells were lysed and probed for the presence of NR1-1a and NR2A. The *lines* under *panels A* and *B* indicate a 10-min exposure of the immunoblot, the *other panels* were exposed to film for 1 min. *B*, following a similar induction protocol, cells were lysed at the times indicated and immunoprecipitated for NR1-1a, and the immunoprecipitates were analyzed for the presence of NR2A. *C*, membranes were prepared from induced L(tk−) cells at the times indicated and analyzed for the presence of oligomeric NMDA receptor subunits using the anti-NR1-1a antibody. *D*, to test the time for association of NR1-1a and NR2A, L(tk−) cells were induced for 24 h and incubated with [^{35}S]methionine for 15 min, before being lysed and immunoprecipitated for NR1-1a. The immunoprecipitate was analyzed on polyacrylamide gels followed by autoradiography.

software using its analysis of variance software and the Kruskal-Wallis test.

RESULTS

Time Course of NR1-1a and NR2A Subunit Synthesis and Association—Whole cell lysates were prepared at the indicated times after cell induction of NMDA receptor synthesis following dexamethasone treatment, and then analyzed using SDS-PAGE. The resulting immunoblot showed that synthesis of the NR1-1a subunits could be detected as early as 1 h after induction while NR2A could be detected in the cell lysates by 2 h (Fig. 1*A*). This difference in the apparent later appearance of the NR2A subunit could reflect a lower detection threshold for the antibody recognizing NR2A, but 2 h after induction both subunits could be readily detected.

The time course of NR1-1a and NR2A subunit association was examined by immunoprecipitating L(tk−) cell lysates with a NR1-1a C-terminal antibody at timed intervals after induction of the cells by dexamethasone. The precipitates were analyzed by immunoblotting with the NR2A antibody to determine whether this subunit co-immunoprecipitated with the NR1-1a subunit. Stable NR1-1a and NR2A subunit association was readily detected 5 h after induction with a weak signal for NR2A visible at 4 h (Fig. 1*B*). Taking into account the possibility that the detection of NR2A may be less sensitive than that of NR1-1a, this result suggests that subunit association can be detected at 4 h following the start of receptor synthesis. We investigated the oligomerization of NR1-1a and NR2A subunits in membranes prepared from the L(tk−) cell line at the indicated timed intervals after induction of receptor synthesis and analyzed using the nondenaturing BN-PAGE system. The resulting immunoblots showed that oligomers with an apparent molecular mass of 860 kDa containing both NR1-1a and NR2A subunits, comparable to the oligomers formed in NR1-1a/NR2A transiently transfected HEK-293 cells as described previously (see Ref. 23), can be detected 6 h after induction of the cells (Fig. 1*C*).

When cells already synthesizing the NMDA receptor are pulse labeled with [^{35}S]methionine for 15 min, then immunoprecipitated for the NR1-1a subunit, the NR2A subunit can be co-immunoprecipitated (Fig. 1*D*). This finding suggests that in cells already expressing the NMDA receptor subunits, newly synthesized NR2A can readily associate with NR1-1a. This result contrasts with our observation that co-immunoprecipitation of NR2A with NR1-1a occurs only after 4 or 5 h of induction, when both subunits have been present for 2 or 3 h. The delay in the association of NR1 and NR2 following induction could either reflect the time taken to synthesize and fold sufficient of each to allow their association, or the time needed for a stable pool of NR1 to form and provide a template for subunit association. We therefore examined further the stability of the individual NR1-1a, NR2A, and NR3A subunits when expressed alone in transiently transfected cells.

NR1 Folds and Dimerizes, whereas NR2 and NR3 Show Aggregation When Expressed Alone—Unfolded proteins often have free cysteines that can cause aggregation of the proteins under nonreducing SDS-PAGE conditions. Therefore, we analyzed the behavior of NR1-1a, NR2A, and NR3A on both nonreduced and reduced gels. The results showed that NR1-1a and NR2A, when individually expressed, yielded predominantly single immunoreactive bands on nonreduced gels that, in the case of NR1-1a, migrated significantly faster than under reducing conditions (Fig. 2). This increase in mobility in the nonreduced samples is due to the interchain disulfide bonds in the folded, or partially folded, protein, which results in a more compact structure than the fully unfolded reduced samples. NR3A, by contrast, consistently gave a range of higher molecular weight bands under nonreducing conditions, suggesting that it is not completely folded when expressed alone (Fig. 2).

To further examine the subunits for free cysteines the short range sulfhydryl-reactive cross-linker BMH was used to treat cells expressing each of the subunits, and the resulting products analyzed on SDS-PAGE gels. NR1-1a consistently migrated as a

monomer and dimer band following BMH treatment of cell lysates (Fig. 3*A*). Similar bands were also seen when rat primary cultures of cortical neurons were treated with BMH (Fig. 3*D*). This suggests that NR1-1a has a limited number of free cysteines and that the subunit may exist as a dimer in the cells, as suggested by our previous studies using BN-PAGE (23). Interestingly, truncation of the C terminus of NR1-1a abolishes this dimer formation, indicating that it must be formed by the cross-linking of its single C-terminal cysteine residue (Fig. 3*B*). BMH treatment of lysates from cells expressing NR2A yielded a more complex pattern with a significant loss of the monomeric form and the production of multiple high molecular weight aggregates (Fig. 3*A*). The C terminus of NR2A contains multiple cysteines that could drive this aggregation, so two truncated versions of NR2A were produced that contained either one or three free cysteines, termed NR2AΔ848 and NR2AΔ890, respectively. Treatment of these with BMH also yielded multiple high molecular weight aggregates and a loss of the monomeric form (Fig. 3*B*). Noticeably, even in the absence of BMH there was evidence of aggregation of the truncated NR2A proteins, possibly due to their high levels of expression. Because the NR2A truncations have reduced numbers of free cysteines, the BMH data suggest that the cross-linking of the proteins must be due to cysteines in the N-terminal domain. NR3A consistently showed almost complete aggregation when treated with BMH (Fig. 3*A*). Because it has only one cysteine at the C terminus this must reflect the presence of multiple free cysteines elsewhere in its sequence, including those found in its different transmembrane regions. The heterogeneity of aggregation of NR2A and NR3A following BMH treatment is in striking contrast with the behavior of NR1-1a and could suggest that the former are being cross-linked not only to themselves but also to intimately associated proteins such as chaperones.

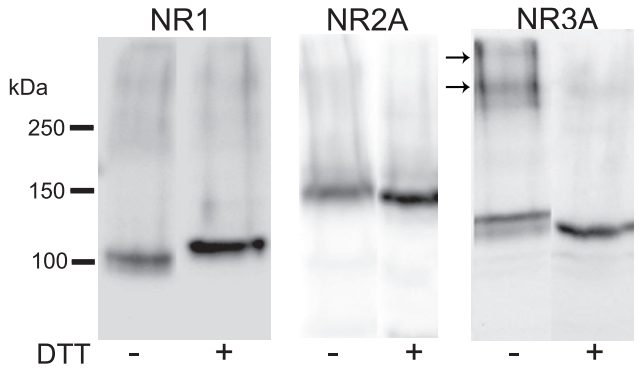

FIGURE 2. **Analysis of HEK-293 cell lysates expressing either NR1-1a, NR2A, or NR3A under nonreduced or reduced conditions.** The lysates from transfected HEK-293 cells were analyzed in the presence (+), or absence (−) of dithiothreitol (*DTT*, 20 mM). Although the presence of dithiothreitol did not affect the behavior of NR2A, nonreduced NR1-1a migrated noticeably faster than when reduced. The *arrows* indicate the presence of the high molecular mass bands in the nonreduced NR3A sample. The faint lower bands visible in the nonreduced *NR1-1a* and *NR3A lanes* may indicate the presence of a nonglycosylated form of the proteins.

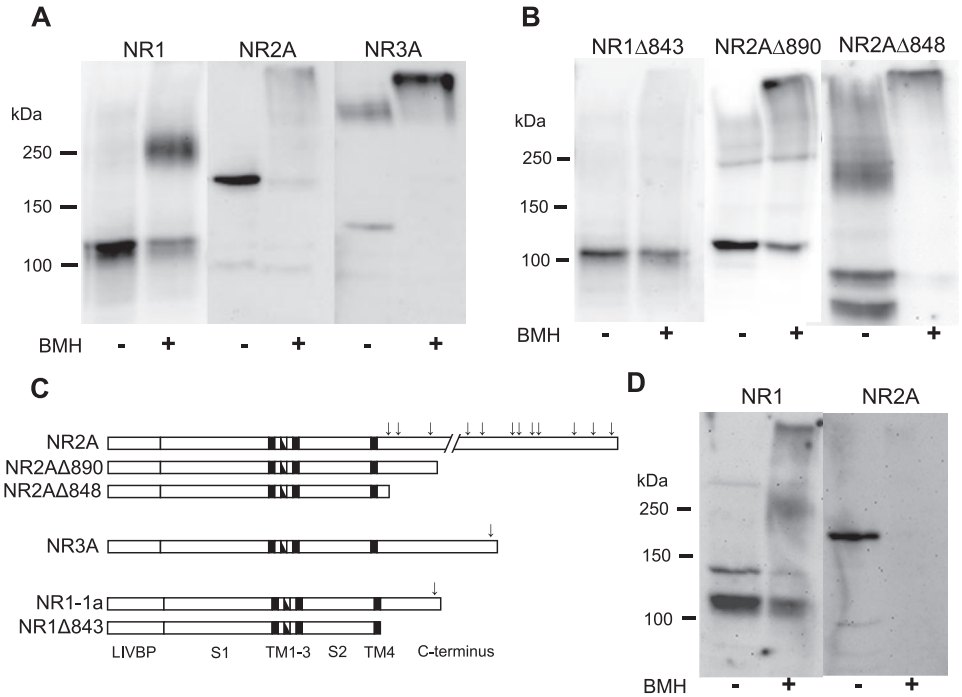

FIGURE 3. **Effect of the sulfhydryl-specific cross-linker BMH on cell lysates from cells expressing NR1-1a, NR2A, and NR3A and rat cortical neurons in culture.** After transfection (24 h) cells expressing the indicated NMDA receptor subunits were lysed in the presence or absence of BMH. *A*, cross-linking of the full-length subunits shows that NR1-1a forms a dimer under these conditions, whereas both NR2A and NR3A tend to form multiple higher oligomers. *B*, because NR2A has multiple cysteines in its C terminus (indicated by the *arrows* in *C*), truncations were performed to reduce these and to remove the single cysteine in the C terminus of NR1-1a. Cross-linking of these mutants shows that NR1-1a no longer gives a dimer, but that both the truncations of NR2A still form multiple high molecular mass oligomers. *D*, cross-linking of cultured rat cortical neuron lysates shows the presence of the NR1 dimer, and that after cross-linking NR1-1a also gives a very high molecular mass band at the top of the gel. NR2A appears to disappear, probably because of the formation of very high molecular mass aggregates, formed from extensive cross-linking of it with NR1 and other proteins in these cells, which do not enter the gel.

Diffusion Rates after ATP Depletion Suggest Misfolding of NR2 and NR3 When Expressed Alone—Unfolded (or partially folded) proteins with free cysteines can show altered diffusion rates in the endoplasmic reticulum when the cells are depleted for ATP due to the prevention of the detachment of chaperone proteins (32). Therefore, the diffusion of YFP-tagged versions of the NMDA receptor subunits was examined in COS-7 cells following depletion of ATP by monitoring FRAP. In control cells, NR1-1a, NR2A, and NR3A had similar diffusion rates and mobile fractions. Although the diffusion of NR1-1a was slightly reduced after ATP depletion, the diffusion of NR3A was significantly reduced, as was its mobile fraction (Fig. 4, *A* and *B*). Full-length NR2A could not be used in this analysis as ATP depletion caused an aggregation of the protein in the cells (see Fig. 4*C*). However, the truncated NR2AΔ890 subunit was analyzed and showed a signifi-

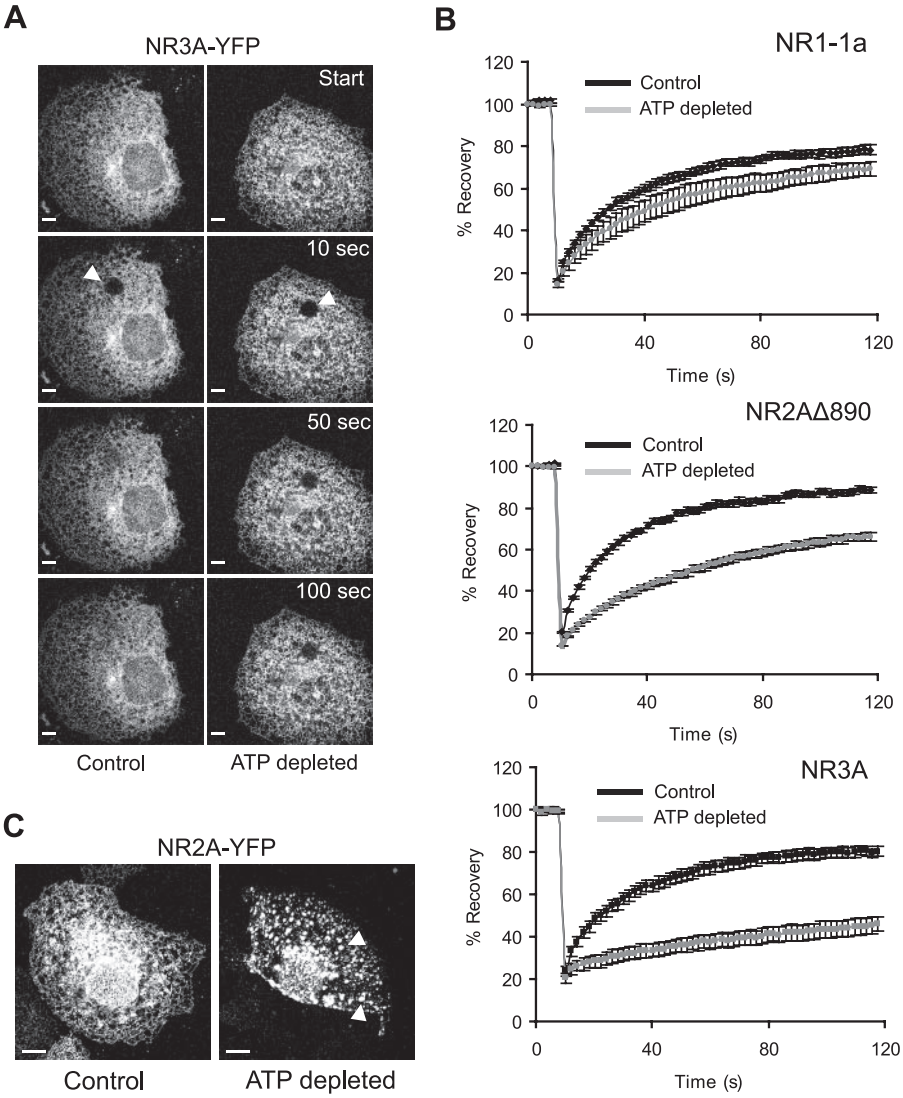

FIGURE 4. **FRAP analysis of COS-7 cells expressing the indicated NMDA receptor subunits.** Mobility of the subunits in the ER of transfected COS-7 was determined 24 h after transfection by FRAP, in cells that were untreated, or treated with 2-deoxyglucose and sodium azide to deplete their ATP levels. *A*, representative images, taken at the indicated times, of NR3A transfected cells. *B*, recovery curves for each subunit. The time to half-maximal recovery ($t_{1/2max}$), and the mobile fractions for the three subunits in untreated cells were: NR1-1a (17.5 ± 1.1 s; 74.2 ± 1.8%), NR2AΔ890 (14.9 ± 1.3 s; 84.6 ± 3.6%), and NR3A (17.5 ± 1.9 s; 77.5 ± 2.7%). Following ATP depletion there was no significant change in these parameters for NR1-1a. However, after ATP depletion NR2AΔ890 showed a significant increase in its $t_{1/2max}$ to 35.8 ± 4.2 s ($p < 0.001$) and a decrease in its mobile fraction to 68.3 ± 3.2% ($p < 0.05$). ATP depletion increased the $t_{1/2max}$ of NR3A to 44.6 ± 3.7 s ($p < 0.001$) and reduced its mobile fraction to 35.1 ± 5% ($p < 0.001$). The results are the mean recoveries from at least ten cells ± S.E., and similar results were obtained in three separate experiments. *C*, ATP depletion causes full-length NR2A subunit to form intracellular inclusions. The *arrows* in *A* indicate the bleached area of the cell; those in *C* highlight the intracellular inclusions of NR2A. The *scale bar* is 10 μm.

cant reduction in its ER diffusion rate with a slight reduction in its mobile fraction (Fig. 4*B*). Taken together, our data are consistent with the hypothesis that NR1 is relatively well folded when expressed alone, whereas NR2 and NR3 are only partially folded, with NR3 possibly less so than NR2.

NR2 and NR3, but Not NR1, Are Rapidly Degraded When Expressed Alone, with NR2 Showing Stabilization in the Presence of NR1—Unfolded proteins often show greater turnover due to their degradation by the proteasome system (33). If NR2 and NR3 were only partially folded when expressed alone, then they should degrade faster than NR1, which appears to be relatively well folded. The degradation rate of the different subunits was therefore examined in cells treated with cycloheximide to block protein synthesis. The results show that NR1-1a has a small (35%) fast degrading component with a half-life of 2.14 h but that, overall, 65% of the protein is stable in the cells (Fig. 5*A*). NR2A and NR3A, however, turn over with half lives of 5.7 and 2.8 h, respectively, with only ~25% of each protein remaining after 24 h. This indicates that NR2A and NR3A are actively degraded and that NR3A is more rapidly degraded than NR2A. If NR1-1a was important for the stabilization of NR2A and NR3A, then co-expression of NR1-1a with these subunits should slow their degradation. In cells co-expressing NR1-1a with NR2A we found that indeed the degradation of NR2A was slowed in the presence of NR1 and, furthermore, the degradation rate of NR2A was similar to that seen in rat cortical neurons in culture (Fig. 5*B*). Surprisingly, co-expression of NR1 with NR3A had little effect on the turnover of the NR3A subunit (Fig. 5*C*). The turnover of NR1 itself was relatively consistent in the differently transfected cells, is similar to that seen in cultured rat cortical neurons (data not shown), and appears independent of the presence of the NR2 and NR3 subunits. Treatment of the cells with lactacystin, an inhibitor of the proteasome system, prevented this turnover of the subunits, with NR2A and NR3A levels significantly increased compared with levels of NR1-1a (Fig. 5*D*).

NR1 Associates with NR2 and NR3, whereas NR2 and NR3 Do Not Associate—To examine the possible range of subunit associations the different subunits were immunoprecipitated when they were expressed alone and when co-expressed. NR1 appears to form stable dimers, as demonstrated by our BN-PAGE and BMH experiments. Expression of NR2A and *myc*-tagged NR2AΔ890 followed by immunoprecipitation of the *myc*-tagged form yielded a small amount of full-length NR2A, suggesting a low level of self-association (Fig. 6). Immunoprecipitation of an HA-tagged version of NR3A when co-expressed with an YFP-tagged form of the subunit failed consistently to give any co-immunoprecipitation of this subunit, suggesting that NR3 does not self-associate. Co-expression of NR1-1a with NR2A or NR3A consistently yielded co-precipitation of the different

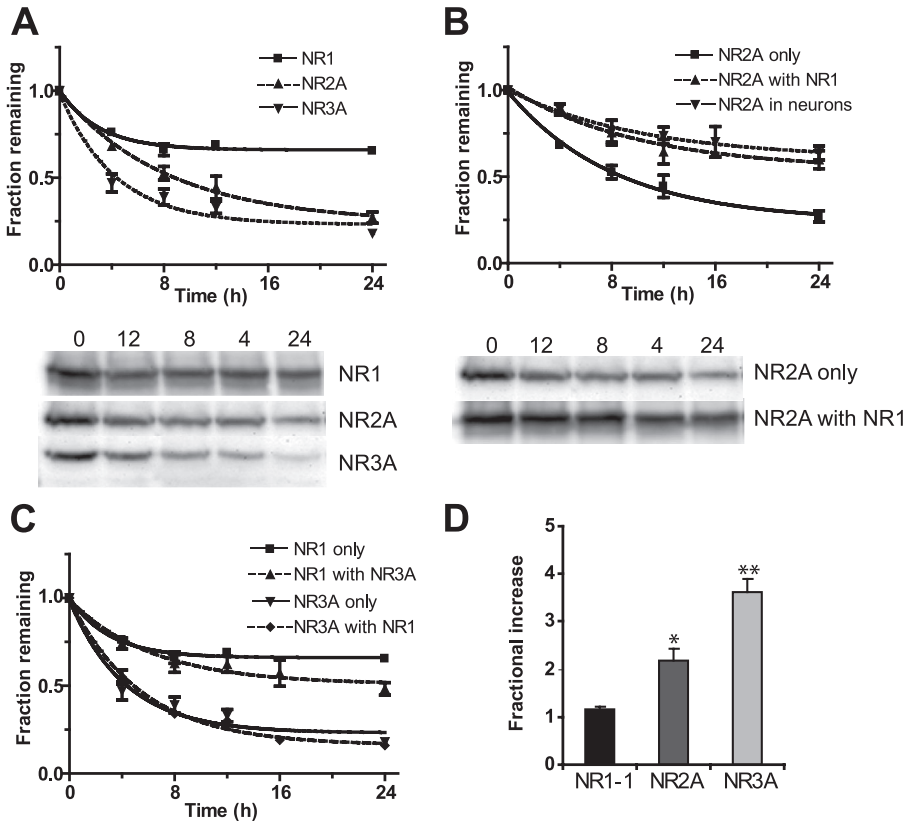

FIGURE 5. **Degradation rates of NR1-1a, NR2A, and NR3A when expressed alone or in combination.** Transfected HEK-293 cells were treated with cycloheximide and analyzed at indicated times. *A*, the NR1-1a subunit degrades more slowly than either NR2A or NR3A. *B*, when co-expressed with NR1-1a, the NR2A subunit becomes more stable with a turnover rate similar to that seen in cultured cortical neurons. *C*, in contrast, co-expression with NR1-1a did not appear to affect turnover of NR3A. Representative immunoblots from separate experiments are shown *below the graphs* in *A* and *B*, probed for the indicated NMDA receptor subunit. Each *graph* represents the pooled data from three separate experiments and the *points* are shown as the mean ± S.E. of six determinations for each time point. The results for the degradation are presented normalized to the level of each subunit at the onset of the experiment. *D*, 16-h treatment of transfected HEK-293 cells with lactacystin caused significant accumulation of NR2A and NR3A over NR1-1a. The results represent the ratio given by the level of the different subunits present in the treated cells divided by that in the untreated cells. Data presented as means ± S.E., *, $p < 0.05$; **, $p < 0.005$ *versus* NR1-1a group.

subunits, as has been reported previously (12, 25). However, NR2A and NR3A did not co-immunoprecipitate (Fig. 6). Thus, although NR2 and NR1 may form dimers, complexes of NR3+NR3 and NR2+NR3 could not be detected under the conditions used here.

DISCUSSION

To date, little is known about the time course of NMDA receptor assembly. Using the inducible expression system of human NR1-1a and NR2A in L(tk−) cells, we have shown that the subunits are rapidly expressed within 2–3 h of induction and that the receptor is an oligomer within 5 h of induction. Despite the early appearance of the two subunits, there is a delay of 2–3 h before they can be co-immunoprecipitated. Although some of this delay could be due to a combination of the different immunodetection thresholds for the two subunits and their having different rates of synthesis or degradation, it could also reflect the time needed for the folding of the subunits before they can stably associate. However, the metabolic labeling studies indicate that the subunits can associate relatively quickly (Fig. 1*D* and Ref. 25). Thus the delay between the induction of the synthesis of the subunits and their ability to be co-immunoprecipitated could also represent the time taken to establish a stable folded pool of NR1 to act as a substrate for further receptor assembly.

Studies on the behavior of the different subunits on polyacrylamide gels run under reducing or nonreducing conditions, together with the sulfhydryl cross-linking experiments, are consistent with the NR1-1a subunit being folded and forming a dimer, whereas NR2A and NR3A contain multiple free cysteines. Although it is possible that the increase in molecular weight of NR1-1a following BMH treatment could be due to cross-linking to other proteins in the endoplasmic reticulum, there is additional evidence to suggest that it can dimerize when expressed alone. Thus we have previously reported that NR1-1a migrates as a dimer on native polyacrylamide gels (23), and this finding is consistent with the necessary formation of an NR1–NR1 disulfide bond for successful trafficking of the receptor to the cell surface (24). Both here, and in the study by Papadakis *et al.* (24), the majority of NR1 appeared as a monomer on nonreducing gels, but the fact that BMH can cross-link it suggests that NR1 forms stable dimers in the ER. Additional evidence for this comes from a fluorescence resonance energy transfer study of the NMDA receptor subunits, in which a fluorescence resonance energy transfer signal was found between appropriately tagged NR1 subunits, even when these were expressed alone (34). The apparent dimerization of NR1-1a following cross-linking must be due to its single C-terminal cysteine, because the truncated form does not form the dimer in the presence of BMH.

Although the aggregation of NR2A when treated with BMH could be due to the cross-linking of its multiple C-terminal cysteines, there are greatly reduced numbers of C-terminal cysteines in its truncated versions, NR2AΔ890 and NR2AΔ848, as well as none in their transmembrane regions. The results obtained with those must therefore be due to the presence of multiple free cysteines in the LIVBP, S1 and S2 domains, consistent with their incomplete folding. The interpretation of the nonreduced gel and cross-linking results from NR3A are complicated by the fact that, although it contains only one C-terminal cysteine, it has four free cysteines in its transmembrane regions and one in the loop between TM2 and TM3 that could contribute to its aggregation after cross-linking or when run on

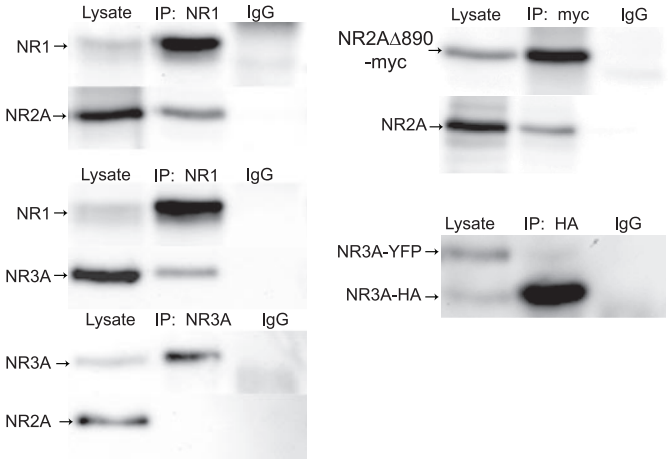

FIGURE 6. **Co-immunoprecipitation of the different combinations of NMDA receptor subunits.** HEK-293 cells were transfected with the indicated NMDA receptor subunits and after 24 h processed for immunoprecipitation. Each *panel* represents a single pair of transfections and contains the lysate (*Lysate*) immunoblotted for the different subunits, the specific immunoprecipitate (*IP*), and a control immunoprecipitate (*IgG*). The *Lysate lane* represents 1/20 of the total material immunoprecipitated. The antibody used in the immunoprecipitation is indicated *above each panel*, and those used for the probe of the immunoblot are at the *left hand side* of *each panel*. NR1-1a co-transfected with NR2A or NR3A gives robust co-immunoprecipitation of the other subunits, whereas NR3A does not give detectable co-immunoprecipitation of NR2A. Analysis of cells co-transfected with the *myc*-His-tagged NR2AΔ890 and NR2A revealed some co-immunoprecipitation of NR2A when the immunoprecipitation was performed with an anti-*myc* antibody. However, co-expression of NR3-YFP with an HA-tagged NR3A, followed by immunoprecipitation with an anti-HA antibody, did not give detectable co-immunoprecipitation of NR3-YFP. Similar results were obtained in three separate experiments.

nonreduced gels. However, to prevent unwanted disulfide bonding, all samples prepared under nonreducing conditions contained 20 mM iodoacetamide to block free cysteines. Therefore, the behavior of NR3A on the nonreduced gels suggests that most of its multimerization had occurred within the cells, again consistent with it not being fully folded. It is worth noting that the different subunits show different behaviors on the unreduced gels, with both NR1-1a and NR2A showing little evidence of aggregation, until BMH treated, whereas NR3A clearly formed aggregates even in the absence of BMH.

If the NMDA receptor subunits were not fully folded, then they might be expected to be degraded rapidly. Although NR1-1a has a fast degrading component (35%; $t_{1/2}$, 2.1 h), the majority (65%) of this subunit is stable over longer time periods. In contrast, both NR2A and NR3A are rapidly degraded with half lives of 5.7 and 2.8 h, respectively. Co-expression of NR1-1a with NR2A increased the stability of the latter, but even when co-expressed with NR1-1a, NR3A was rapidly degraded. Interestingly, the degradation of NR2A and NR1-1a, when co-expressed, were comparable to the rates observed for these subunits in rat cortical cultures. In a study of rat cerebellar granule cells, NR1 was also seen to have a pool of rapidly turned over NR1, and NR2 was found to be relatively stable in the presence of NR1 (35). Failure to stabilize NR3A by co-expressing it with NR1-1A may reflect either the relative inefficiency of forming stable NR1-1a/NR3A receptors or the rapid turnover of these in HEK 293 cells compared with the NR1-1a/NR2A receptors.

Altered rates of ER diffusion in ATP-depleted cells have, at least for some proteins, been shown to depend on the formation of mixed disulfide bonds with ER-resident chaperones (32, 36). These protein complexes require ATP to break the mixed disulfide bonds and free the proteins to diffuse freely, so that when cells are ATP-depleted the ER diffusion of unfolded or misfolded proteins tends to slow (32). Our diffusion data are consistent with the idea that NR1-1a is more completely folded and stable relative to either NR2A or NR3A, because the diffusion of the latter two subunits, but not of NR1-1a, is significantly more reduced in cells depleted for ATP. Here too the behavior of the NR3A subunit shows a different behavior from either NR1-1a or NR2A, with a more profound block of diffusion on ATP depletion.

In the present study we show that NR1-1a was readily immunoprecipitated with NR2A and NR3A, but that NR2A showed weak self-association and NR2A-NR3A or NR3A-NR3A complexes were not detectable. The failure, in this study, to co-immunoprecipitate NR2 and NR3 is in contrast to the results obtained in two other reports (12, 37). This could reflect the use of the human subunits here, rather than the rat subunits used in the other studies, or methodological differences such as our inclusion of iodoacetamide in the cell lysates to prevent non-specific disulfide bond formation. Our results are also largely consistent with the subunit association data obtained by the analysis of the fluorescence resonance emission transfer between NR1 and NR2 subunits, which showed that NR1 and NR2 expressed alone appeared to associate, as they did when co-expressed (34). The NR3 subunit was not examined in these studies. We note that, although we show evidence for some homodimerization of NR2A, in view of the degradation studies reported here, the dimer formed must be relatively unstable.

Stable folding of NR1 in the absence of other subunits is necessary if it is to act as a substrate for the stable assembly of the NMDA receptor. The reported observation that NR1 alone can form a glycine binding site suggests that it can fold well when expressed alone in mammalian cells (5, 9). It also forms a glycine binding site when produced in mammalian or insect cells as a soluble protein by fusion of the S1–S2 domain (23, 38–40). In contrast, there is little evidence that NR2 can similarly fold when expressed alone, with one report of glutamate binding to NR2A (41), while others found either little glutamate binding (42) or a failure of glutamate antagonist binding (43). However, co-expression of NR1 with NR2 subunits produces robust glutamate binding, and indeed all studies on residues influencing glutamate binding have been achieved using co-expression systems (10, 11, 44). Further evidence for the importance of NR1 and NR2 association comes from the observation that the glycine affinity of the NR1 subunit is increased by association with NR2, suggesting an allosteric effect of this subunit association on the tertiary structure of NR1 (42).

A central role for the NR1 subunit in NMDA receptor folding and assembly could explain the reported excess of NR1 in the brain and neurons (45, 46). For example, there is a large pool of NR1 in the cytoplasm of cerebellar granule cells (35). This pool of NR1 could be ready to recruit and fold the NR2 and NR3 subunits as they are synthesized. Reduced levels of NR1 would be expected to decrease NR2 and NR3 levels if NR1 was necessary for the stability and further folding of NR2 or NR3. Indeed, in a conditional NR1 knock-out mouse model, where the tar-

geted brain area was the CA1 region of the hippocampus, the levels of both NR2A and NR2B proteins were significantly reduced, but the amount of NR2A or NR2B mRNA was not affected (47).

Taken together, the data presented here show that the different NMDA receptor subunits, when expressed alone, behave differently with respect to their stability, susceptibility to sulfhydryl cross-linking agents, and diffusion in the absence of ATP, consistent with the interpretation that NR1-1a is stably folded, whereas NR2A and NR3A are less so. These data have implications for models of NMDA receptor assembly and support the central role of the NR1 subunit in the assembly of the NMDA receptor, where it may provide a stable substrate for the folding and oligomerization of the receptor.

Acknowledgment—We thank Dr. Peter Wingrove for providing the NR3A constructs and his invaluable help in the production of some of the other constructs used here.

REFERENCES

1. Dingledine, R., Borges, K., Bowie, D., and Traynelis, S. F. (1999) *Pharmacol. Rev.* **51,** 7–61
2. Sun, L., Margolis, F. L., Shipley, M. T., and Lidow, M. S. (1998) *FEBS Lett.* **441,** 392–396
3. Ciabarra, A. M., Sullivan, J. M., Gahn, L. G., Pecht, G., Heinemann, S., and Sevarino, K. A. (1995) *J. Neurosci.* **15,** 6498–6508
4. Nishi, M., Hinds, H., Lu, H. P., Kawata, M., and Hayashi, Y. (2001) *J. Neurosci.* **21,** RC185
5. Grimwood, S., Le Bourdelles, B., and Whiting, P. J. (1995) *J. Neurochem.* **64,** 525–530
6. Cik, M., Chazot, P. L., and Stephenson, F. A. (1993) *Biochem. J.* **296,** 877–883
7. Varney, M. A., Jachec, C., Deal, C., Hess, S. D., Daggett, L. P., Skvoretz, R., Urcan, M., Morrison, J. H., Moran, T., Johnson, E. C., and Velicelebi, G. (1996) *J. Pharmacol. Exp. Ther.* **279,** 367–378
8. Kuryatov, A., Laube, B., Betz, H., and Kuhse, J. (1994) *Neuron* **12,** 1291–1300
9. Hirai, H., Kirsch, J., Laube, B., Betz, H., and Kuhse, J. (1996) *Proc. Natl. Acad. Sci. U. S. A.* **93,** 6031–6036
10. Laube, B., Hirai, H., Sturgess, M., Betz, H., and Kuhse, J. (1997) *Neuron* **18,** 493–503
11. Anson, L. C., Chen, P. E., Wyllie, D. J. A., Colquhoun, D., and Schoepfer, R. (1998) *J. Neurosci.* **18,** 581–589
12. Perez-Otano, I., Schulteis, C. T., Contractor, A., Lipton, S. A., Trimmer, J. S., Sucher, N. J., and Heinemann, S. F. (2001) *J. Neurosci.* **21,** 1228–1237
13. Chatterton, J. E., Awobuluyi, M., Premkumar, L. S., Takahashi, H., Talantova, M., Shin, Y., Cui, J. K., Tu, S. C., Kevin, A. S. K., Nakanishi, N., Tong, G., Lipton, S. A., and Zhang, D. X. (2002) *Nature* **415,** 793–798
14. Awobuluyi, M., Yang, J., Ye, Y., Chatterton, J. E., Godzik, A., Lipton, S. A., and Zhang, D. (2007) *Mol. Pharmacol.* **71,** 112–122
15. Madry, C., Mesic, I., Bartholomaus, I., Nicke, A., Betz, H., and Laube, B. (2007) *Biochem. Biophys. Res. Commun.* **354,** 102–108
16. Greger, I. H., Khatri, L., and Ziff, E. B. (2002) *Neuron* **34,** 759–772
17. Ayalon, G., and Stern-Bach, Y. (2001) *Neuron* **31,** 103–113
18. Tichelaar, W., Safferling, M., Keinanen, K., Stark, H., and Madden, D. R. (2004) *J. Mol. Biol.* **344,** 435–442
19. Armstrong, N., Sun, Y., Chen, G. Q., and Gouaux, E. (1998) *Nature* **395,** 913–917
20. Furukawa, H., Singh, S. K., Mancusso, R., and Gouaux, E. (2005) *Nature* **438,** 185–192
21. Furukawa, H., and Gouaux, E. (2003) *EMBO J.* **22,** 2873–2885
22. Schorge, S., and Colquhoun, D. (2003) *J. Neurosci.* **23,** 1151–1158
23. Meddows, E., LeBourdelles, B., Grimwood, S., Wafford, K., Sandhu, S., Whiting, P., and McIlhinney, R. A. J. (2001) *J. Biol. Chem.* **276,** 18795–18803
24. Papadakis, M., Hawkins, L. M., and Stephenson, F. A. (2004) *J. Biol. Chem.* **279,** 14703–14712
25. McIlhinney, R. A. J., Le Bourdellès, B., Molnár, E., Tricaud, N., Streit, P., and Whiting, P. L. (1998) *Neuropharmacology* **35,** 1355–1367
26. Garside, M. (2005) in *Physiological Sciences*, pp. 181–192, University of Oxford, Oxford
27. Grimwood, S., Lebourdelles, B., Atack, J. R., Barton, C., Cockett, W., Cook, S. M., Gilbert, E., Hutson, P. H., Mckernan, R. M., Myers, J., Ragan, C. I., Wingrove, P. B., and Whiting, P. J. (1996) *J. Neurochem.* **66,** 2239–2247
28. Chan, W. Y., Soloviev, M. M., Ciruela, F., and McIlhinney, R. A. J. (2001) *Mol. Cell Neurosci.* **17,** 577–588
29. Schagger, H., Cramer, W. A., and von Jagow, G. (1994) *Anal. Biochem.* **217,** 220–230
30. Schagger, H., and von Jagow, G. (1991) *Anal. Biochem.* **199,** 223–231
31. Esapa, C. T., Waite, A., Locke, M., Benson, M. A., Kraus, M., McIlhinney, R. A., Sillitoe, R. V., Beesley, P. W., and Blake, D. J. (2007) *Hum. Mol. Genet.* **16,** 327–342
32. Nehls, S., Snapp, E. L., Cole, N. B., Zaal, K. J., Kenworthy, A. K., Roberts, T. H., Ellenberg, J., Presley, J. F., Siggia, E., and Lippincott-Schwartz, J. (2000) *Nat. Cell Biol.* **2,** 288–295
33. Goldberg, A. L. (2003) *Nature* **426,** 895–899
34. Qiu, S., Hua, Y. L., Yang, F., Chen, Y. Z., and Luo, J. H. (2005) *J. Biol. Chem.* **280,** 24923–24930
35. Huh, K. H., and Wenthold, R. J. (1999) *J. Biol. Chem.* **274,** 151–157
36. Esapa, C. T., McIlhinney, R. A., and Blake, D. J. (2005) *Hum. Mol. Genet.* **14,** 295–305
37. Matsuda, K., Fletcher, M., Kamiya, Y., and Yuzaki, M. (2003) *J. Neurosci.* **23,** 10064–10073
38. Miyazaki, J., Nakanishi, S., and Jingami, H. (1999) *Biochem. J.* **340,** 687–692
39. Ivanovic, A., Reilander, H., Laube, B., and Kuhse, J. (1998) *J. Biol. Chem.* **273,** 19933–19937
40. Neugebauer, R., Betz, H., and Kuhse, J. (2003) *Biochem. Biophys. Res. Commun.* **305,** 476–483
41. Kendrick, S. J., Lynch, D. R., and Pritchett, D. B. (1996) *J. Neurochem.* **67,** 608–616
42. Laurie, D. J., and Seeburg, P. H. (1994) *Eur. J. Pharmacol. Mol. Pharmacol. Section* **268,** 335–345
43. Lynch, D. R., Anegawa, N. J., Verdoorn, T., and Pritchett, D. B. (1994) *Mol. Pharmacol.* **45,** 540–545
44. Kinarsky, L., Feng, B., Skifter, D. A., Morley, R. M., Sherman, S., Jane, D. E., and Monaghan, D. T. (2005) *J. Pharmacol. Exp. Ther.* **313,** 1066–1074
45. Chazot, P. L., and Stephenson, F. A. (1997) *J. Neurochem.* **68,** 507–516
46. Hall, R. A., and Soderling, T. R. (1997) *J. Biol. Chem.* **272,** 4135–4140
47. Fukaya, M., Kato, A., Lovett, C., Tonegawa, S., and Watanabe, M. (2003) *Proc. Natl. Acad. Sci. U. S. A.* **100,** 4855–4860